Friction-induced torsional vibrations in an experimental drill-string system

Friction-Induced Torsional Vibrations in an Experimental Drill-String System

N. Mihajlović, A. A. van Veggel, N. van de Wouw, H. Nijmeijer
Eindhoven University of Technology
Department of Mechanical Engineering
Dynamics and Control Group
Den Dolech, PO Box 513
5600 MB Eindhoven, The Netherlands
tel: +31 40 247 {4850, 4580, 3358, 3203}, fax: +31 40 246 1418
e-mail: {N.Mihajlovic, A.A.v.Veggel, N.v.d.Wouw, H.Nijmeijer}@tue.nl

ABSTRACT
In this paper, we aim for an improved understanding of the causes for torsional vibrations in rotary drilling systems that are used for the exploration of oil and gas. For this purpose, an experimental drill-string set-up is considered. In that system, torsional vibrations with and without stick-slip are observed in steady-state. In order to obtain a predictive model, a discontinuous static friction model is used. The parameters of the suggested model are estimated and the steady-state behaviour of the drill-string system is analysed both numerically and experimentally. A comparison of numerical and experimental bifurcation diagrams indicates the predictive quality of the model. Moreover, specific friction model characteristics can be linked to the existence of torsional vibrations with and without stick-slip.

KEY WORDS
Discontinuous friction model, bifurcation diagram, nonlinear system, parameter estimation, torsional vibrations

1 Introduction

Deep wells for the exploration and production of oil and gas are drilled with a rotary drilling system. A rotary drilling system creates a borehole by means of a rock-cutting tool, called a bit. The torque driving the bit is generated at the surface by a motor with a mechanical transmission box. Via the transmission, the motor drives the rotary table: a large disc that acts as a kinetic energy storage unit. The medium to transport the energy from the surface to the bit is a drill-string, mainly consisting of drill pipes. The lowest part of the drill-string is the Bottom-Hole-Assembly consisting of drill collars and the bit. The drill-string undergoes various types of vibrations during drilling: torsional (rotational) vibrations, caused by nonlinear interaction between the bit and the rock or the drill-string and the borehole wall; bending (lateral) vibrations, often caused by pipe eccentricity, leading to centripetal forces during rotation; axial (longitudinal) vibrations, due to bouncing of the drilling bit on the rock during rotation; hydraulic vibrations in the circulation system, stemming from pump pulsations.

Drill-string vibrations are an important cause for premature failure of drill-string components and drilling inefficiency. In this paper, torsional drill-string vibrations are investigated. Since the behaviour of the system when a constant torque is applied at the rotary table of a drill-string system is of interest, the focus is on the steady-state behaviour of drill-string systems for such constant torques.

Extensive research on the subject of torsional vibrations has already been conducted [2, 5, 10, 11, 12, 13, 14, 18]. According to some of those results, the cause for torsional vibrations is the stick-slip phenomenon due to the friction force between the bit and the well [10, 12, 13]. Moreover, the cause for torsional vibrations can be the negative damping in the friction force present due to the contact between the bit and the borehole, see for example [2, 11]. In order to gain an improved understanding of the causes for torsional vibrations, an experimental drill-string set-up is built. The set-up consists of a DC-motor which is connected to the upper disc via a gear box. The upper and lower disc are connected via a low stiffness string and at the lower disc an additional brake is applied. In the set-up, torsional vibrations with and without stick-slip are observed and the behaviour of the set-up is analysed. However, using existing friction models which are used for modelling torsional vibrations in drill-string systems [10, 11, 12, 13] not all steady-state phenomena, observed in the experimental drill-string system, can be modelled. Using another discontinuous static friction model, those experimentally observed phenomena are successfully predicted. In such a friction model, positive damping is present for very small angular velocities, for higher angular velocities, negative damping occurs and for even higher angular velocities positive damping is again present in the friction [3, 4, 8, 9]. In [3, 4], such a friction model is called “humped friction model”. It follows that both in the model and the experiments the steady-state behaviour undergoes various qualitative changes when the input voltage is changed. These changes are typically captured in a bifurcation diagram that features the changes of equilibrium

points into limit cycling (vibrations). A comparison of the numerical and experimental bifurcation diagram illustrates the predictive quality of the suggested model. Moreover, such a bifurcation diagram provides improved insight in how torsional vibrations in drill-string systems are created.

In Section 2, the experimental drill-string set-up is described. Next, the dynamic behaviour of the set-up is modelled and the parameters of the model are estimated. In the experimental system as well as in the estimated model both equilibria (constant velocity) and limit cycles (torsional vibrations) are observed when a constant input torque is applied. Therefore, in Section 3, the equilibrium point (set) is determined and related stability properties are discussed. Next, periodic solutions and their stability properties are determined numerically. Subsequently, based on the proposed model and estimated parameters, a bifurcation diagram is presented and compared to experimentally obtained results. In Section 4, conclusions are presented.

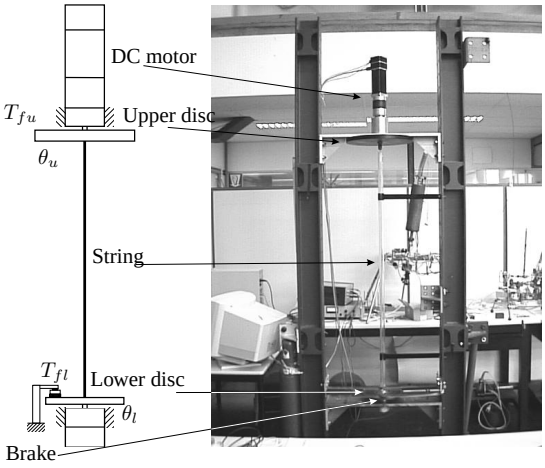

Figure 1. Experimental drill-string set-up.

2 Drill-String Set-Up

2.1 Experimental Set-Up

The experimental drill-string set-up is shown in Figure 1. The input voltage from the computer, which is between $-5\,\mathrm{V}$ and $5\,\mathrm{V}$, is fed into the DC-motor via the power amplifier. The DC-motor, which represents the drive motor of a real drill rig, is connected, via the gear box, to the upper steel disc (which represents the rotary table of the rig). The upper and lower disc are connected through a low stiffness steel string. The drill-string and the lower brass disc represent the drill-string with the Bottom-Hole-Assembly at the real drill-rig and the additional brake represents the friction force between the drill bit and borehole. The contact material of the brake is rubber. The angular positions of the upper and lower disc are measured using incremental encoders. The angular velocities of both discs are obtained by numerical differentiation of the angular positions and filtering the resulting signals using a low-pass filter. In Figure 1, as well as further on in the text, θ_u and θ_l are the angular positions of the upper and lower disc, respectively, T_{fu} is the friction torque present in the motor and in the bearings at the upper disc and T_{fl} represents the friction torque at the lower disc which is caused by the friction between lower disc and the brake and by the friction in the bearings.

2.2 Model of the Set-Up

The drill-string set-up is an electro-mechanical system and it can be described by:

$$\begin{aligned} J_u\ddot{\theta}_u + k_\theta(\theta_u - \theta_l) + T_{fu}(\dot{\theta}_u) &= k_m\, u \\ J_l\ddot{\theta}_l - k_\theta(\theta_u - \theta_l) + T_{fl}(\dot{\theta}_l) &= 0, \end{aligned} \tag{1}$$

where u is the input voltage to the power amplifier of the motor, J_u and J_l are moments of inertia of the upper and lower disc with respect to the center of the mass, respectively, k_θ is the torsional stiffness of the string and k_m is the motor constant. In (1), friction torques T_{fu} and T_{fl} are modelled by

$$\begin{aligned} T_{fu}(\dot{\theta}_u) &\in \begin{cases} T_u(\dot{\theta}_u)\mathrm{sign}(\dot{\theta}_u) & \text{for} \quad \dot{\theta}_u \neq 0, \\ [-T_u(0), T_u(0)] & \text{for} \quad \dot{\theta}_u = 0, \end{cases} \\ T_{fl}(\dot{\theta}_l) &\in \begin{cases} T_l(\dot{\theta}_l)\mathrm{sign}(\dot{\theta}_l) & \text{for} \quad \dot{\theta}_l \neq 0, \\ [-T_l(0), T_l(0)] & \text{for} \quad \dot{\theta}_l = 0, \end{cases} \end{aligned} \tag{2}$$

which represent set-valued friction laws[1]. The nonlinear functions $T_u(\dot{\theta}_u)$ and $T_l(\dot{\theta}_l)$ represent friction torques present at the upper and lower disc for non-zero angular velocities and for those nonlinear functions the following holds:

$$T_u(\dot{\theta}_u),\ T_l(\dot{\theta}_l) \geq 0,\ \forall\, \dot{\theta}_u,\ \dot{\theta}_l \in \mathbb{R}, \tag{3}$$

which means that the friction torques in (2) are dissipative.

The reason for using a set-valued function to model the friction at the upper and lower disc is the fact that both at the upper and at the lower disc the stiction phenomenon is observed experimentally. Moreover, (2) indicates that the friction torques are modelled using a static friction model. This choice is based on the following reasoning: we are interested in the steady-state behaviour of the set-up and we are not interested in a detailed dynamic modelling of the friction for very small angular velocities.

The dynamics of the fourth-order system (1), can be described by a third-order state-space system since its dynamics is independent of the angular positions of the discs but only depends on the difference between these two angular positions. Therefore, by choosing state coordinates $x_1 = \theta_u - \theta_l$, $x_2 = \dot{\theta}_u$ and $x_3 = \dot{\theta}_l$, the following state-

[1] With the set $[a,\ b]$ we mean the interval $\{x \in \mathbb{R} \mid a \leq x \leq b\}$.

space model can be obtained

$$\begin{aligned}\dot{x}_1 &= x_2 - x_3,\\ \dot{x}_2 &= \tfrac{k_m}{J_u}u - \tfrac{k_\theta}{J_u}x_1 - \tfrac{1}{J_u}T_{fu}(x_2),\\ \dot{x}_3 &= \tfrac{k_\theta}{J_l}x_1 - \tfrac{1}{J_l}T_{fl}(x_3).\end{aligned} \quad (4)$$

This model is used for further analysis of the dynamic behaviour of the drill-string set-up.

2.3 Parameter Estimation and Friction Modelling

In order to obtain a predictive model of the drill-string set-up, the parameters k_m, J_u, J_l, k_θ and nonlinear functions $T_u(\dot{\theta}_u)$ and $T_l(\dot{\theta}_l)$ need to be estimated.

First, the upper disc is disconnected from the lower disc and the parameters concerning the motor and the upper disc (k_m, J_u and $T_u(\dot{\theta}_u)$) are estimated. The estimation process is based on dedicated experiments involving responses of the system, when constant input voltages u are applied, and an identification procedure ensuring a close match between the model predictions and experimental results (see for example [7]). The estimated parameters indicate that the friction torque at the upper disc is asymmetric ($T_{fu}(\dot{\theta}_u) \neq -T_{fu}(-\dot{\theta}_u)$) and that no Stribeck effect is present. Therefore, the friction torque T_{fu} in (2) is modelled with

$$T_u(\dot{\theta}_u) = T_{su} + \triangle T_{su}\text{sign}(\dot{\theta}_u) + b_u|\dot{\theta}_u| + \triangle b_u\dot{\theta}_u, \quad (5)$$

where $T_{su} + \triangle T_{su}$ and $-T_{su} + \triangle T_{su}$ represent the maximum and minimum value of the friction torque for zero angular velocities and $b_u + \triangle b_u$ and $b_u - \triangle b_u$ are viscous friction coefficients present for positive and negative velocities, respectively. The identification porcedure yields the following parameter values:

$$\begin{aligned}&J_u = 0.4765\,\tfrac{\text{kg m}^2}{\text{rad}},\ k_m = 3.5693\,\tfrac{\text{Nm}}{\text{V}},\\ &T_{su} = 0.3212\,\text{Nm}\ \triangle T_{su} = 0.0095\,\text{Nm},\\ &b_u = 1.9833\tfrac{\text{kg m}^2}{\text{rad s}},\ \triangle b_u = -0.0167\tfrac{\text{kg m}^2}{\text{rad s}}.\end{aligned} \quad (6)$$

In order to gain improved insight in the causes for torsional vibrations in real drilling systems, an additional brake is applied to the lower disc of the experimental drill-string set-up. The brake material is rubber. For several levels of the normal force applied to the brake, no torsional vibrations in steady-state are observed when a constant input voltage is applied. However, when water is added between the lower brass disc and the contact material of the brake, torsional steady-state vibrations appear for constant input voltages. Moreover, both torsional vibrations with and without stick-slip behaviour appear[2]. In [10, 12, 13], it is stated that torsional vibrations in drill-string systems can be modelled using the friction model with the Stribeck effect. However, using such model, only torsional vibrations *with* stick-slip can been modelled. Therefore, a humped friction model, as shown in figure 2, is used. The difference between the humped friction model and the friction model with only the Stribeck effect is evident for low angular velocities. Namely, in the humped friction model, positive damping is present for very small angular velocities which is not the case for friction with only the Stribeck effect.

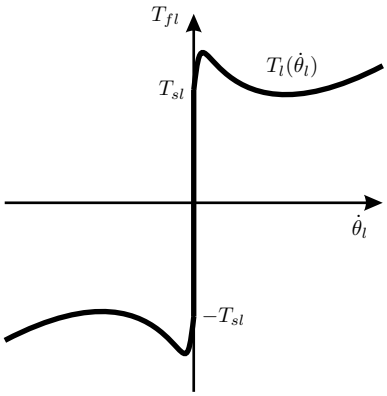

Figure 2. Humped friction model.

Based on a Neural Network model [6, 7, 15] the friction torque T_{fl}, as in figure 2, can be expressed by friction model (2) with:

$$\begin{aligned}T_l(\dot{\theta}_l) = T_{sl} &+ T_1\left(1 - \tfrac{2}{1+e^{\beta_1|\dot{\theta}_l|}}\right)\\ &+T_2\left(1 - \tfrac{2}{1+e^{\beta_2|\dot{\theta}_l|}}\right) + b_l|\dot{\theta}_l|,\end{aligned} \quad (7)$$

where T_{sl}, T_1, T_2, β_1, β_2, b_l are parameters of the friction model. Moreover, $-T_{sl}$ and T_{sl} represent the minimum and the maximum static friction level, respectively and b_l is the viscous friction coefficient.

In order to estimate the remaining parameters of the set-up (k_θ, J_l, T_{sl}, T_1, T_2, β_1, β_2, b_l), a quasi-random voltage signal is applied to the motor. Next, using nonlinear least-square algorithm, the parameters are estimated by ensuring a close match between the measured and simulated angular position of the lower disc $\dot{\theta}_l$. The obtained estimates are:

$$\begin{aligned}&J_l = 0.0326\,\tfrac{\text{kg m}^2}{\text{rad}},\ k_\theta = 0.078\,\tfrac{\text{Nm}}{\text{rad}},\\ &T_{sl} = 0.00940\,\text{Nm},\ b_l = 0.0042\,\tfrac{\text{kg m}^2}{\text{rad s}},\\ &T_1 = 0.0826\,\text{Nm},\ T_2 = -0.291\,\text{Nm},\\ &\beta_1 = 6.3598\,\tfrac{\text{s}}{\text{rad}},\ \beta_2 = 0.0768\,\tfrac{\text{s}}{\text{rad}}.\end{aligned} \quad (8)$$

A validation procedure is performed using different input signals such as a quasi-random (see figure 3), harmonic, constant, ramp and parabolic signals. For those signals, the comparison between the responses of the experimental set-up and estimated model indicates the accuracy of the obtained parameters and the predictive quality of the resulting model (see also Section 3).

[2] More about friction phenomenon due to a contact between two materials can be found in [1, 3, 8, 9].

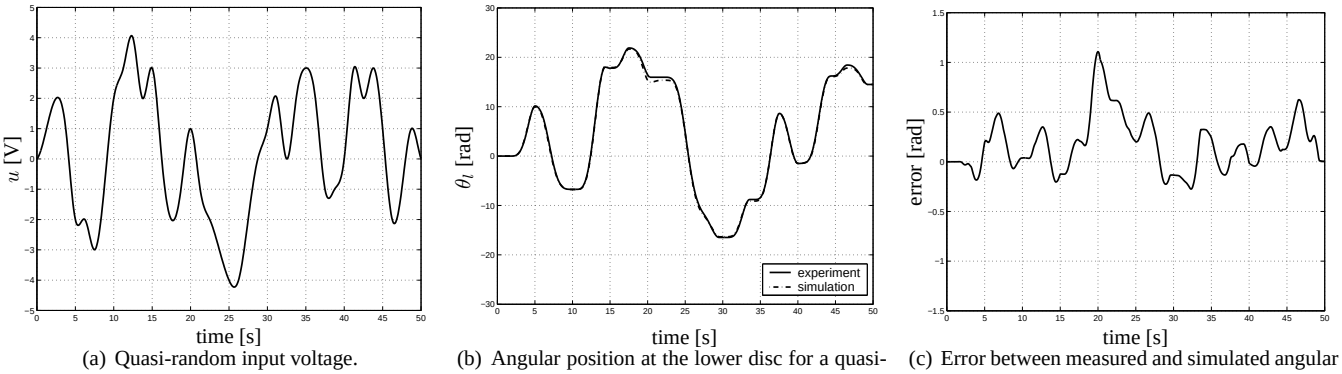

(a) Quasi-random input voltage.

(b) Angular position at the lower disc for a quasi-random input signal.

(c) Error between measured and simulated angular position at the lower disc for a quasi-random input signal.

Figure 3. Validation signals for the drill-string set-up.

3 The Steady-State Behaviour of the Set-Up

Both equilibria (constant velocity at both the upper and lower disc) and limit cycles (torsional vibrations at the lower disc) are observed in the experimental set-up. In this section, the stability of both the equilibrium points (sets) and the limit cycles of the model are investigated. Moreover, the model results are compared with the experimental results.

3.1 Equilibrium points

In the equilibrium points it holds that $(x_1,\, x_2,\, x_3) = (x_{1eq},\, x_{2eq},\, x_{3eq})$, for $u = u_c$, with u_c a constant, and x_{1eq}, x_{2eq}, x_{3eq} satisfy

$$\begin{aligned} &x_{2eq} - x_{3eq} = 0, \\ &k_m u_c - T_{fu}(x_{3eq}) - T_{fl}(x_{3eq}) = 0, \\ &k_\theta x_{1eq} - T_{fl}(x_{3eq}) = 0. \end{aligned} \tag{9}$$

According to the analysis of the equilibrium points of the model of the set-up (equations (1), (2), (5) and (7)) with the estimated parameters (6) and (8), the bifurcation diagram shown in figure 4 is constructed[3].

First, for $u_c \leq u_{c1}$, $u_{c1} = (T_{su} + \triangle T_{su} + T_{sl})/k_m$ (point A in figure 4), the system is in the stiction phase and the equilibrium points $\mathbf{x}_{eq} = (x_{1eq},\, 0,\, 0)$ of the system are such that $\mathbf{x}_{eq} \in \mathcal{E}$, where $\mathcal{E}$ represents the equilibrium *set* defined by:

$$\begin{aligned} \mathcal{E} = \Big\{ \mathbf{x} \in \mathbb{R}^3 \;\Big|\; & x_1 \in \left[\tfrac{-T_{sl}}{k_\theta},\, \tfrac{T_{sl}}{k_\theta} \right] \\ & \cap \left[\tfrac{k_m u_c - T_{su} - \triangle T_{su}}{k_\theta},\, \tfrac{k_m u_c + T_{su} - \triangle T_{su}}{k_\theta} \right], \\ & x_2 = 0,\; x_3 = 0 \Big\}. \end{aligned} \tag{10}$$

Both the lower and the upper disc do not rotate (the equilibrium set satisfies $x_{2eq} = x_{3eq} = 0$) due to the fact that input voltage is not big enough to drive the upper and lower disc. Moreover, using Lyapunov stability theory it is possible to prove that the equilibrium set (10) is locally asymptotically stable (see [14, 19]). Those equilibrium sets are denoted as equilibrium branch e_1 in the constructed bifurcation diagram in figure 4. Next, for $u_c > u_{c1}$ system has a unique equilibrium point, such that $x_{2eq} = x_{3eq} > 0$, which is the solution of the following nonlinear algebraic equation:

$$\begin{aligned} &x_{2eq} = x_{3eq}, \\ &k_m u_c - (b_u + \triangle b_u) x_{3eq} - T_{su} - \triangle T_{su} \\ &- T_l(x_{3eq}) = 0, \\ &x_{1eq} = \tfrac{T_l(x_{3eq})}{k_\theta}. \end{aligned} \tag{11}$$

In order to obtain local stability conditions for this equilibrium point, the nonlinear system (4) is linearized around the equilibrium point. According to the Routh-Hurwitz criterion, the equilibrium point of system (4) is locally asymptotically stable for

$$d_l > -0.00114\, \frac{\mathrm{kg\,m}}{\mathrm{rad\,s}}, \tag{12}$$

with

$$d_l = \tfrac{\mathrm{d}T_l}{\mathrm{d}x_3}\big|_{x_3 = x_{3eq}} \tag{13}$$

the (linearized) friction damping present at the lower disc when angular velocity is $\dot{\theta}_l = x_{3eq}$ and the estimated system parameters (6) and (8). Given the fact that for very low but non-zero velocities positive damping is present in the friction torque at the lower disc (see figure 2), it can be concluded that an asymptotically stable equilibrium branch e_2 exists (see figure 4). If u_c increases, the corresponding solution x_{3eq} increases as well. For u_c large enough, the friction damping d_l does not satisfy condition (12) any more and the system has an *unstable* equilibrium point (equilibrium branch e_3 in figure 4). For even larger u_c, the system has a locally asymptotically stable equilibrium point (equilibrium branch e_4 in figure 4). In point A of the bifurcation

[3] For the simplicity, the steady-state analysis is performed only for $u_c > 0$.

diagram in figure 4 no change of stability properties occurs. Moreover, the locally asymptotically stable equilibrium set e_1, defined by (10), merges into the locally asymptotically stable equilibrium branch e_2. In points B and D a change in stability properties occurs. Namely, a pair of complex conjugate eigenvalues, related to the linearisation of the nonlinear dynamics of (4) around the equilibrium point, cross the imaginary axis to the right-half complex plane. Therefore, Hopf bifurcations occur at these points [17].

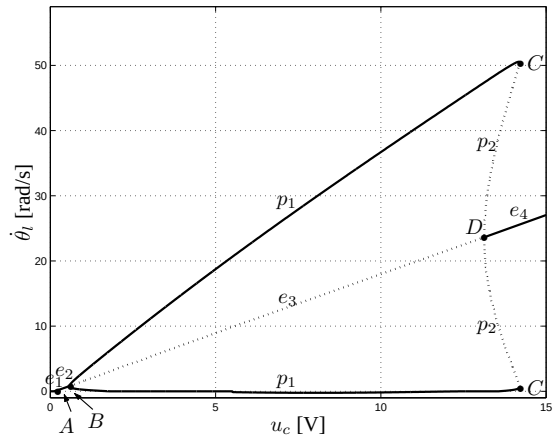

Figure 4. Bifurcation diagram of the drill-string set-up.

3.2 Periodic Solutions

Next, using a path following technique in combination with a shooting method [16], limit cycles are computed numerically for the estimated model of the system and the results are shown in the bifurcation diagram in figure 4. In that figure, the maximal and minimal values of x_3 are plotted when a limit cycle is found. Floquet multipliers, corresponding to these limit cycles, are computed numerically and used to determine the local stability properties of these limit cycles. Although the estimated friction torque at the lower disc, when the brake is used, is not considered to be accurate for $u_c > 5\,\mathrm{V}$, the bifurcation diagram is determined as well in order to understand the behaviour of the set-up for higher constant input voltages. With respect to the obtained results the following remarks can be made:

From bifurcation point B, a stable periodic branch p_1 arises. Moreover, close to the bifurcation point, the periodic branch p_1 consists of limit-cycles which represent torsional vibrations without stick-slip. Therefore, bifurcation point B represents a smooth supercritical Hopf bifurcation point. If we analyse the bifurcation diagram in figure 4, it can be noticed that the periodic branch p_1 consists of limit-cycles which represents torsional vibrations without stick-slip when $\min(x_3) > 0$ and with stick-slip ($\min(x_3) = 0$). For even higher u_c, the locally stable periodic branch p_1 looses its stability and an unstable periodic branch appears (periodic branch p_2 in figure 4). The point where the stable periodic branch p_1 is connected to the unstable branch p_2 represents a fold bifurcation point (point C in figure 4). The unstable periodic branch p_2 is connected to the equilibrium branches e_3 and e_4 in a subcritical Hopf bifurcation point D.

3.3 Experimental Results

In order to check the validity of the obtained model of the drill-string set-up, experimental results are compared with the numerical results. As already mentioned, the evidence about the predictive quality of the estimated model in steady-state is of great interest. Therefore, the same type of bifurcation diagram, as shown in figure 4, is constructed experimentally. In order to construct such an experimental bifurcation diagram, different constant input voltages are applied to the set-up. When no torsional vibrations are observed, the mean value of the recorded angular velocity is computed. Next, when torsional vibrations are observed at the lower disc, the mean value of local maxima and minima are computed as well. Then, all experimentally obtained data for constant input voltages are plotted using the symbol "o" in figure 5. Since the input voltage is limited to $5\,\mathrm{V}$, the experimental data are available only up to $u_c = 5\,\mathrm{V}$. According to the results, shown in figures 3 and 5, it can be concluded that: the equilibrium sets (equilibrium branch e_1), the equilibrium points (equilibrium branche e_2), a Hopf bifurcation point (point B) the magnitude of the limit cycles (periodic branch p_1) and the dynamic behaviour of the set-up (see figure 3) are well predicted.

Consequently it can be concluded that the observed torsional vibrations are caused by the nonlinearity present in the friction at the lower disc and such nonlinearity is modelled adequately using the friction model shown in figure 2. Figure 5 shows that the amplitude of the vibrations depends on the applied constant input voltage while the period time shows only small changes. Moreover, when the period time of the the vibrations is analysed, it is noticed that the observed vibrations is very close to the period time of the linear resonance frequency of the set-up.

4 Conclusions

In this paper, the dynamic model of the set-up is introduced, the parameters of the set-up are estimated and the steady state-behaviour of a drill-string set-up is analysed in order to investigate the cause for torsional vibrations. In the set-up, when brake is used at the lower disc, torsional vibrations with and without stick-slip are observed in steady-state. Torsional stick-slip vibrations in drill-string systems can be predicted using a static friction model with the Stribeck effect [10, 11, 12, 13]. However, torsional vibrations without stick-slip cannot be modelled using the same friction model. Therefore, a humped discontinuous

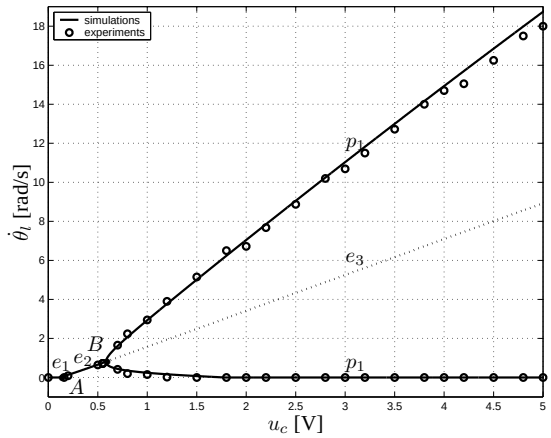

Figure 5. Simulated and experimental (circles) bifurcation diagram of the drill-string set-up.

static friction model [3, 4, 8, 9] is used. The difference between the humped friction model and a friction model with only the Stribeck effect is that for very small angular velocities the proposed friction model has a positive damping. With such model, the observed torsional vibrations in the experimental set-up, both with and without stick-slip, are successfully predicted. As a result of the steady-state analysis, a bifurcation diagram, with constant input voltage u_c as a bifurcation parameter, is presented. Moreover, a comparison between the numerical and experimental bifurcation diagrams illustrates the predictive quality of the suggested model.

References

[1] Armstrong-Hélouvry, B., Amin, B., 1994, A Survey of Models, Analysis Tools and Compensation Methods for the Control of Machines with Friction, *Automatica*, 30(7), pp. 1083-1138.

[2] Brett, J. F., 1992, The Genesis of Torsional Drillstring Vibrations, *SPE Drilling Engineering*, pp. 168-174.

[3] Brockley, C. A., Cameron, R., Potter, A. F., 1967, Friction-Induced Vibration, *Transactions of ASME: Journal of Lubrication Technology*, 89, pp. 101-108.

[4] Brockley, C. A., Ko, P. L., 1970, Quasi-Harmonic Friction-Induced Vibration, *Transactions of ASME: Journal of Lubrication Technology*, 92, pp. 550-556.

[5] Cunningham, R. A., 1968, Analysis of Downhole Measurements of Drill String Forces and Motions, *Transactions of ASME: Journal of Engineering for Industry*, 90, pp. 208-216.

[6] Hensen, R. H. A., Angelis, G. Z., Molengraft v. d., M. J. G., Jager d., A. G., Kok, J. J., 2000, Grey-box modeling of friction: An experimental case-study, *European Journal of Control*, 6 (3), pp. 258-267.

[7] Hensen, R. H. A., 2002, *Controlled Mechanical Systems with Friction*, Ph.D. Thesis, Eindhoven University of Technology, Eindhoven, The Netherlands.

[8] Ibrahim, R. A., 1994, Friction-induced vibration, chatter, squeal, and chaos; Part I: Mechanics of contact and friction, *Transactions of ASME: Applied Mechanics Reviews*, 47(7), pp. 209-226.

[9] Ibrahim, R. A., 1994, Friction-induced vibration, chatter, squeal, and chaos; Part II: Dynamics and modeling, *Transactions of ASME: Applied Mechanics Reviews*, 47(7), pp. 227-253.

[10] Jansen, J. D., van de Steen, L., 1995, Active Damping of Self-Excited Torsional Vibrations in Oil Well Drillstrings, *Journal of Sound and Vibration*, 179(4), pp. 647-668.

[11] Kust, O., 1998, *Selbsterregte Drehschwingungen in schlanken Torsionssträngen: Nichtlineare Dynamik und Regelung*, Ph.D. Thesis, Techincal University Hamburg-Harburg, Germany.

[12] Leine, R. I., 2000, *Bifurcations in Discontinuous Mechanical Systems of Filippov-Type*, PhD Thesis, Eindhoven University of Technology, Eindhoven, The Netherlands.

[13] Leine, R. I., van Campen, D. H., Keultjes, W. J. G., 2002, Stick-slip Whirl Interaction in Drillstring Dynamics, *Transactions of ASME: Journal of Vibrations and Acoustics*, 124, pp. 209-220.

[14] Mihajlović, N., Van Veggel, A. A., Van de Wouw, N., Nijmeijer, H., (2003), Analysis of Friction-Induced Limit Cycling in an Experimental Drill-String Set-Up, submitted to *ASME Journal of Dynamic Systems, Measurements and Control*.

[15] Narendra, K. S., Parthasarathy, K., 1990, Identification and Control of Dynamical Systems Using Neural Networks, *IEEE Transactions on Neural Networks*, 1, pp. 4-27.

[16] Parker, T. S., Chua, L. O., *Practical Numerical Algorithms for Chaotic Systems*, Springer-Verlag, 1989.

[17] Sastry, S., 1999, *Nonlinear Systems*, Springer-Verlag, New York, USA.

[18] Tucker, R. W., Wang, C., 1999, An Integrated Model for Drill-String Dynamics, *Journal of Sound and Vibrations*, 224(1), pp. 123-165.

[19] Van de Wouw, N., Leine, R. I., (2003), Attractivity of Equilibrium Sets of Systems with Dry Friction, submitted for publication in *Nonlinear Dynamics*.